PROCEEDINGS OF SCIENCE

Physics updates of the high-energy lepton and photon simulation tool PROPOSAL

Jean-Marco Alameddine,[a,*] **Pascal Gutjahr,**[a] **Wolfgang Rhode,**[a] **Alexander Sandrock**[b] **and Jan Soedingrekso**[a]

[a] *Technische Universität Dortmund, Fakultät Physik,*
Otto-Hahn-Straße 4a, 44227 Dortmund, Germany

[b] *Bergische Universität Wuppertal, Fakultät für Mathematik und Naturwissenschaften,*
Gaußstraße 20, 42119 Wuppertal, Germany

E-mail: `jean-marco.alameddine@tu-dortmund.de`, `pascal.gutjahr@tu-dortmund.de`, `wolfgang.rhode@tu-dortmund.de`, `asandrock@icecube.wisc.edu`, `jan.soedingrekso@tu-dortmund.de`

Monte Carlo simulations are an important tool in modern physics experiments. With improving detector sensitivities, higher accuracies are also required from simulations, for example in reconstruction tasks. This includes both correctness from a physical as well as an algorithmic point of view. PROPOSAL is a Monte Carlo simulation framework that provides three-dimensional simulations of high-energy photons, electrons, muons, and taus. It is written in C++, but can also be used within Python via a wrapper. The structure of the software allows for simple customization of the propagation environment, physics descriptions, or precision settings for a variety of use cases. Examples are the application in neutrino observatories, underground experiments, or air shower simulations. This contribution focuses on the recent physics updates of the framework, describing the methodology and implication of these improvements. In particular, this involves effects at the higher and lower end of the energy scale covered by PROPOSAL. For high-energy photons, photon-nucleon interactions, muon pairproduction, and the Landau-Pomeranchuk-Migdal effect in electron-positron pairproduction are now included. As lower-energy effects, the deflection of muons in stochastic interactions as well as an approximate description of the photoeffect for photons have been implemented.

38th International Cosmic Ray Conference (ICRC2023)
26 July - 3 August, 2023
Nagoya, Japan

PoS(ICRC2023)482

---

[*] Speaker

1. Introduction

Modern experiments in physics rely on methods of statistical data analysis to interpret their measurements. To train these methods, a statistically sufficient dataset where the true properties are known is required. Especially in astroparticle physics, this can only be achieved using simulations which model the reality. One of these simulation tools is the framework PROPOSAL [1], which provides a three-dimensional Monte Carlo simulation of high-energy particles propagating through large volumes[1]. Originally, PROPOSAL has been written for the simulation of muon and tau leptons in the context of underground observatories, such as the IceCube Neutrino Observatory [2], or for radio neutrino detectors [3]. To be able to use PROPOSAL for the simulation of electromagnetic cascades, a recent update introduced pair production and Compton scattering as photon interactions, annihilation as a new positron interaction, and new dedicated parametrizations to describe ionization and bremsstrahlung losses of electrons and positrons [4]. With these updates, PROPOSAL could be used to simulate the electromagnetic component of extensive air showers, as it is done in the air shower simulation framework CORSIKA 8 [5].

In this contribution, the implementation of additional photon interaction processes is presented. This includes photoelectric absorption, photonuclear interactions, muon pair production, and a description of the Landau-Pomeranchuk-Migdal suppression in electron-positron pair production. These processes are important to describe photons as low energies ($E \lessapprox 0.1\,\mathrm{MeV}$ in air) and very-high energies ($E \gtrapprox 10^{18}\,\mathrm{eV}$ in air), as well as due to their distinct event signatures.

2. Physics improvements for photon interactions

2.1 Photoelectric absorption

Photoelectric absorption describes the ejection of an atomic electron due to its interaction with an in-going photon. In this process, the photon energy is used to free the electron from its atomic binding, while the remaining photon energy serves as the kinetic energy of the now free electron. For photons in air, photoelectric absorption becomes the dominant interaction process for energies below $\approx 30\,\mathrm{keV}$. In the context of electromagnetic cascades, photoelectric absorption as a process starts to become important for energies where its cross section represents a significant correction to the total mean free path length.

The detailed description of photoelectric absorption is non-trivial and dependent on the properties interaction target and its atomic structure. Since the energy where photoelectric absorption becomes dominant is small, and the process is not important for the electromagnetic shower development, PROPOSAL only provides an approximate description based on the cross section given in [6, 7]. The total cross section is defined as

$$\sigma = 4\pi r_e^2 Z^5 \alpha^4 F_1 F_2 \left(\frac{m_e}{E}\right)^5 \left(\gamma^2 - 1\right)^{3/2} \left[\frac{4}{3} + \frac{\gamma(\gamma - 2)}{\gamma + 1}\left(1 - \frac{\ln\left(\gamma + \sqrt{\gamma^2 - 1}\right)}{\gamma\sqrt{\gamma^2 - 1}}\right)\right], \tag{1}$$

---

[1] PROPOSAL is available as an open-source C++/Python software under https://github.com/tudo-astroparticlephysics/PROPOSAL. It can be installed with `pip install proposal` or via CMake.

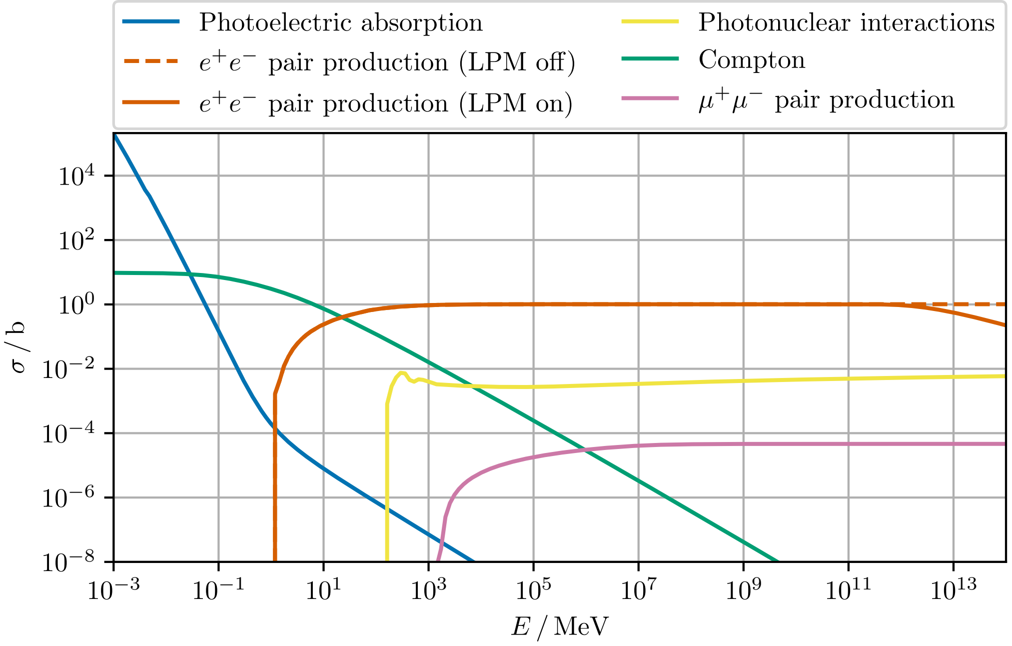

Figure 1: Total cross section of photons in air inside PROPOSAL.

with the photon energy E and the definitions

$$\gamma = 1 + \frac{E - I}{m_e}, \qquad I = \frac{Z^2\alpha^2 m_e}{2}. \tag{2}$$

The term

$$F_1 = \left[1 + \left(\frac{\alpha Z}{\beta}\right)^2\right] \frac{\pi\alpha Z/\beta}{\sinh(\pi\alpha Z/\beta)} \exp\left[\frac{\alpha Z}{\beta}\left(\pi - 4\arctan\left(\frac{\beta}{\alpha Z}\right)\right)\right] \tag{3}$$

is used as a correction factor for the non-relativistic energy regime [7], while the term

$$F_2 = 1 + 0.01481 \ln^2 Z - 0.000788 \ln^3 Z \tag{4}$$

is an empirical correction describing the ratio between the K-shell and total photoelectric absorption cross section [8].

The photoelectric cross section and a validation of the total photon cross section at low energies is shown in Figure 2, where the total photon cross section in air is compared to the calculations from the NIST Standard Reference Database [9]. Since the cross section used to describe the photoelectric effect is only valid for energies large compared to absorption edges, the deviations of up to 10 % in the low-energy regime are expected. This also explains why the K absorption line of argon at $E \approx 3.2 \times 10^{-3}$ MeV is not well described.

2.2 Photonuclear interactions

High-energy photons can perform hadronic interactions, in which the photon is absorbed by an atomic nucleus. Although this process provides only a small contribution to the total mean free

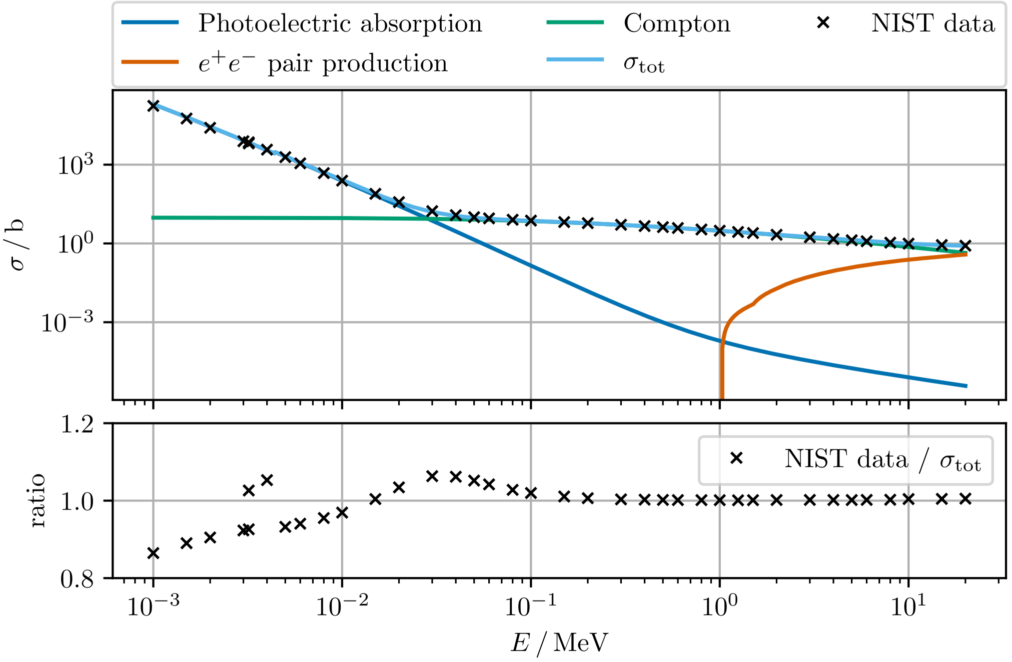

Figure 2: Photon cross sections in air for small energies, compared to the total cross section according to the NIST Standard Reference Database [9].

path length of photons for most energies, they are a source of hadronic particles, and consequently also muons from electromagnetic cascades.

In the context of nuclear muon interactions, parametrizations to describe photonuclear interactions of photons have already been implemented in PROPOSAL, but were only available internally. These parametrization, which have been described in detail in [1], are now available to describe photonuclear interaction of real photons.

In addition, the parametrization from [10], which is also used in the simulation program CORSIKA 7, has also been implemented. The continuous contribution of this cross section is given as

$$\sigma_{\gamma,N} = \begin{cases} \left(73.3s^{0.073} + 191.7s^{-0.602}\right)\sqrt{1 - s_0/s}\,\mu\text{b}, & \text{for } \sqrt{s} \le 19.39\,\text{GeV}, \\ \left(59.3s^{0.093} + 120.2s^{-0.358}\right)\mu\text{b}, & \text{for } \sqrt{s} > 19.39\,\text{GeV}, \end{cases} \tag{5}$$

with $s = m_n^2 + 2m_nE/\text{GeV}$ and the pion production threshold $\sqrt{s_0} = 1.0761\,\text{GeV}$. In addition, the resonances for $\Delta(1232)$, $N(1520)$, and $N(1680)$ are superimposed on the continuous cross section, where the definition and parameters from [11] are used. Figure 3 shows the different parametrizations for the photonuclear interactions implemented in PROPOSAL. Note that both differences in the resonance region as well as in the extrapolation to high energies are visible. Figure 1 shows the cross section of photonuclear interactions compared to other processes. For energies where the LPM suppression of pair production becomes effective, the photonuclear process starts to become a significant contribution to the total photon cross section.

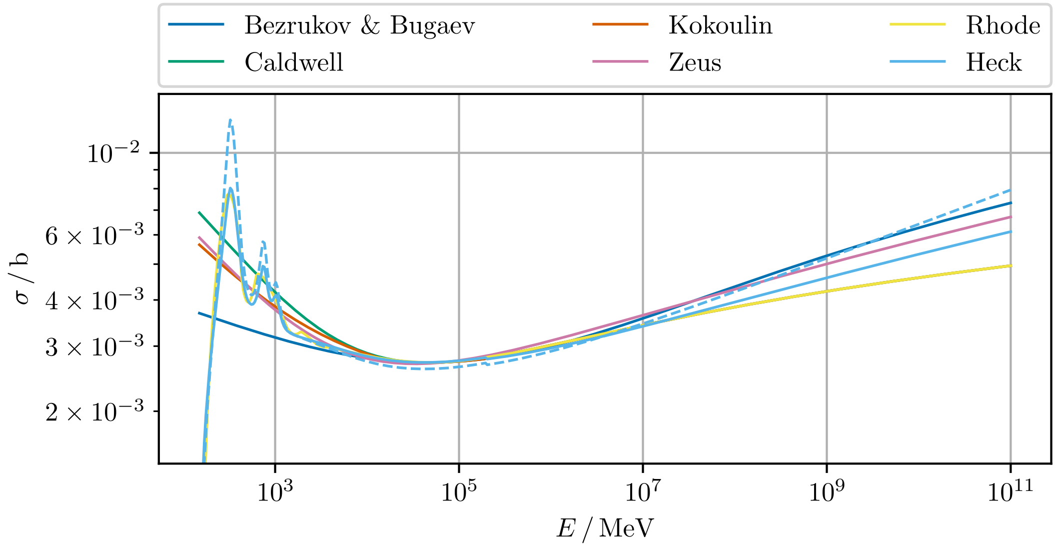

Figure 3: Photonuclear interaction cross sections implemented in PROPOSAL. For the Heck parametrization, the solid line indicates the shadowing parametrization according to [1], while for the dashed line, the shadowing parametrization $\sigma_{\gamma,A} = A^{0.91}\sigma_{\gamma,N}$ from [10] has been used.

2.3 Muon pair production

Muon pair production describes the conversion of a photon to a muon pair in the field of an atomic nucleus. While the contribution of this process to the mean free path length of photons is negligible compared to the dominant electron-positron pair production, it provides a source of muons from the electromagnetic shower component and therefore a potentially interesting event signature in extensive air showers.

Based on the muon bremsstrahlung cross section given in [12], the muon pair production cross section is given by

$$\begin{aligned}\frac{\mathrm{d}\sigma}{\mathrm{d}x} &= 4Z^2\alpha\left(r_e\frac{m_e}{m_\mu}\right)^2\left[1-\frac{4}{3}(x-x^2)\right]\\ &\quad\times\left(\Phi(\delta)+\frac{1}{Z}\left[\ln\left(\frac{m_\mu/\delta}{\delta m_\mu/m_e^2+\sqrt{e}}\right)-\ln\left(1+\frac{1}{\delta\sqrt{e}B'Z^{-2/3}/m_e}\right)\right]\right),\end{aligned} \tag{6}$$

where

$$\Phi(\delta) = \underbrace{\ln\left(\frac{BZ^{-1/3}m_\mu/m_e}{1+BZ^{-1/3}\sqrt{e}\delta/m_e}\right)}_{\Phi_0} - \underbrace{\ln\left(\frac{D_n}{1+\delta(D_n\sqrt{e}-2)/m_\mu}\right)}_{\Delta_\mathrm{n}}, \tag{7}$$

with the radiation logarithm constant B, the inelastic radiation logarithm B', and the definitions

$$x = \frac{E_{\mu^-}}{E}, \qquad \delta = \frac{m_\mu^2}{2Ex(1-x)}, \qquad D_n = 1.54A^{0.27}. \tag{8}$$

For $Z > 1$, the effect of the inelastic nuclear form factor is included with the substitution

$$\Delta_\mathrm{n} \rightarrow \left(1 - \frac{1}{Z}\right) \Delta_\mathrm{n}. \tag{9}$$

The total cross section of muon pair production is shown in Figure 1.

2.4 Landau-Pomeranchuk-Migdal effect in electron-positron pair production

The Landau-Pomeranchuk-Migdal effect is a suppression of bremsstrahlung and pair production processes occuring when the formation length reaches interatomic distances, which comes in effect for high energies and dense media. The suppression is effective for small energy losses in case of bremsstrahlung, and for symmetric pair production events in case of electron-positron pair production.

Based on the parametrization of the LPM effect in [13], the suppression of the pair production cross section is given by

$$\frac{\mathrm{d}\sigma_\mathrm{LPM}}{\mathrm{d}x} = \frac{\mathrm{d}\sigma}{\mathrm{d}x} \cdot \frac{\xi(s)/3 \left(G(s) + 2\left(x^2 + (1-x)^2\right)\phi(s)\right)}{1 - 4/3x(1-x)}, \tag{10}$$

with $x = E_{e^-}/E$, where E is the photon energy. The functions $\xi(s)$, $G(s)$, $\phi(s)$, are given by [14, 15]

$$\xi(s) \approx \xi(s') = \begin{cases} 2 & \text{if } s' < s_1, \\ 1 + h - \frac{0.08(1-h)(1-(1-h)^2)}{\ln(s_1)} & \text{if } s_1 \leq s' < 1, \\ 1 & \text{if } s' \geq 1, \end{cases} \tag{11}$$

$$G(s) = \begin{cases} 3\psi(s) - 2\phi(s) & \text{if } s < 0.710\,390, \\ 36s^2/(36s^2 + 1) & \text{if } 0.710\,390 \leq s < 0.904\,912, \\ 1 - 0.022s^{-4} & \text{if } s \geq 0.904\,912, \end{cases} \tag{12}$$

$$\psi(s) = 1 - \exp\left\{-4s - \frac{8s^2}{1 + 3.936s + 4.97s^2 - 0.05s^3 + 7.5s^4}\right\}, \tag{13}$$

$$\phi(s) = \begin{cases} 1 - \exp\left\{-6s\left(1 + (3-\pi)s\right) + \frac{s^3}{0.623 + 0.796s + 0.658s^2}\right\} & \text{if } s < 1.549\,54, \\ 1 - 0.012s^{-4} & \text{if } s \geq 1.549\,54, \end{cases} \tag{14}$$

with the variable definitions

$$s = \frac{s'}{\sqrt{\xi(s')}}, \qquad s' = \frac{1}{8}\sqrt{\frac{E_\mathrm{LPM}}{Ex(1-x)}}, \qquad s_1 = \frac{\sqrt{2}Z^{2/3}}{B^2}, \tag{15}$$

$$E_\mathrm{LPM} = \frac{2\alpha(m_e c^2)^2 X_0}{\pi\hbar c}, \qquad h = \frac{\ln(s')}{\ln(s_1)}, \qquad D_n = 1.54A^{0.27}, \tag{16}$$

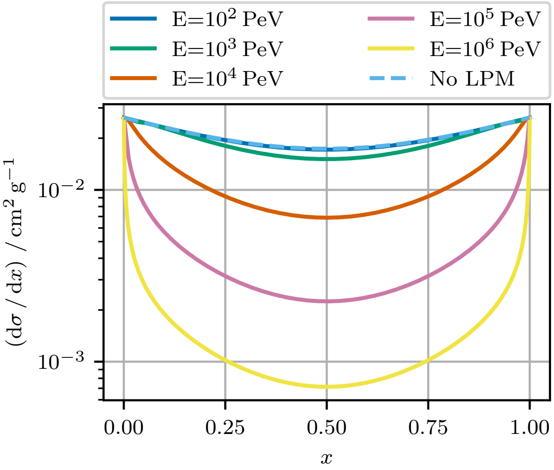

Figure 4: Differential cross section for electron-positron pair production in air at sea level, with nitrogen as an interaction target. The effect of the LPM effect at different energies is shown. Note that without the LPM suppression, the differential cross section is almost identical for all energies in this plot.

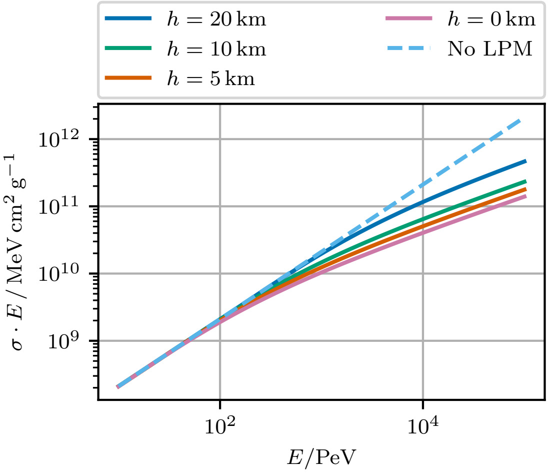

Figure 5: Total cross section for electron-positron pair production in air, with the effect of the LPM suppression at different atmospheric heights.

where X_0 is the radiation length and B the radiation logarithm constant.

Figure 4 shows the effect of the LPM suppression on the differential pair production cross section at different energies. As expected, for $x = 0.5$, the suppression becomes maximal, while for $x \longrightarrow 0$ and $x \longrightarrow 1$, the suppression is zero. Since the LPM effect depends on the material density, its suppression also depends on the height in the Earth's atmosphere. In Figure 5, the suppression of the pair production cross section at different atmospheric heights is shown.

3. Summary and outlook

In this contribution, the implementation of the photoelectric effect, photonuclear interactions, muon pair production, and the LPM effect for pair production as well as the effect of these processes on the total photon cross section have been presented. For photon energies below $\approx 20\,\mathrm{MeV}$, the implementation has been verified by comparison with independent calculations. With these updates, PROPOSAL is now able to provide a complete description of electron, positron, and photon processes in the energy range important for the simulation of electromagnetic cascades. The current main application for these improvements is the air shower simulation framework CORSIKA 8, where the current status is presented in [5]. Other applications are possible as well, due to the modular structure of PROPOSAL. In the future, the simulation of neutrino interactions with PROPOSAL using only-stochastic propagation is planned to be implemented.

Acknowledgments

This work has been supported by the Deutsche Forschungsgemeinschaft (DFG) and the Lamarr institute. Jean-Marco Alameddine acknowledges the financial support by the German Academic Exchange Service (DAAD).

References

[1] J.-H. Koehne, K. Frantzen, M. Schmitz, T. Fuchs, W. Rhode, D. Chirkin et al., *Proposal: A tool for propagation of charged leptons*, Comput. Phys. Commun. **184** (2013) 2070.

[2] R. Abbasi et al., *Improved Characterization of the Astrophysical Muon–neutrino Flux with 9.5 Years of IceCube Data*, Astrophys. J. **928** (2022) 50.

[3] D. García-Fernández, A. Nelles and C. Glaser, *Signatures of secondary leptons in radio-neutrino detectors in ice*, Phys. Rev. D **102** (2020) 083011.

[4] J.-M. Alameddine, J. Alvarez-Muniz, J. Ammerman-Yebra, L. Bollmann, W. Rhode, M. Sackel et al., *Electromagnetic Shower Simulation for CORSIKA 8*, in *Proceedings of 37th International Cosmic Ray Conference — PoS(ICRC2021)*, vol. 395, p. 428, 2021.

[5] J.-M. Alameddine, A. Sandrock and F. Riehn, *Validation of Electromagnetic Showers in CORSIKA 8* , in *Proceedings of 38th International Cosmic Ray Conference — PoS(ICRC2023)*, p. 393, 2023.

[6] W. Heitler, *The Quantum Theory of Radiation*, Clarendon Press, Oxford (1954).

[7] F. Sauter, *Über den atomaren Photoeffekt in der K-Schale nach der relativistischen Wellenmechanik Diracs*, Annalen der Physik **403** (1931) 454 .

[8] J.H. Hubbell, *Photon cross sections, attenuation coefficients, and energy absorption coefficients from 10 keV to 100 GeV*, Tech. Rep. NSRDS-NBS 29, National Bureau of Standards (1969).

[9] J.M. Hubbell and S.M. Seltzer, *Tables of X-Ray Mass Attenuation Coefficients and Mass Energy-Absorption Coefficients from 1 keV to 20 MeV for Elements Z = 1 to 92 and 48 Additional Substances of Dosimetric Interest*, Tech. Rep. NISTIR 5632, National Institute of Standards and Technology (05, 1995).

[10] D. Heck, *Production of Vector Mesons by Photonuclear Interactions in the Program CORSIKA*, Tech. Rep. Forschungszentrum Karlsruhe (2012).

[11] A. Mücke, R. Engel, J. Rachen, R. Protheroe and T. Stanev, *Monte Carlo simulations of photohadronic processes in astrophysics*, Comput. Phys. Commun. **124** (2000) 290.

[12] S.R. Kelner, R.P. Kokoulin and A.A. Petrukhin, *About cross section for high-energy muon bremsstrahlung*, Tech. Rep. MEPHI-95-24 (1995).

[13] S. Klein, *Suppression of bremsstrahlung and pair production due to environmental factors*, Rev. Mod. Phys. **71** (1999) 1501.

[14] T. Stanev, C. Vankov, R.E. Streitmatter, R.W. Ellsworth and T. Bowen, *Development of ultrahigh-energy electromagnetic cascades in water and lead including the Landau-Pomeranchuk-Migdal effect*, Phys. Rev. D **25** (1982) 1291.

[15] A.B. Migdal, *Bremsstrahlung and pair production in condensed media at high energies*, Phys. Rev. **103** (1956) 1811.